



Effect of valve lift at different IVO ,IVC and OVERLAP angles on SI Engine performance.

Kutaeba J.M. AL-Khishali kutaibaal_khishali@yahoo.com University of Technology, Mechanical Engineering Department, Baghdad, Iraq.

Yousef S.H. Najjar y_najjar@hotmail.com Jordan University of Science and Technology, Mechanical Engineering Department, Irbid, Jordan.

Osama H. Ghazal okhazal@philadelphia.edu.jo Philadelphia University, Mechanical Engineering Department, Amman Jordan

Abstract

The effect of variation of valve lift on the performance was studied. The analysis took into consideration the effect of varying the IVO, IVC and Overlap angles. Power, Torque BMEP, BSFC and Volumetric efficiency was estimated as well as the NO and CO emission for all cases considered. As the current emission legislations and the large concern about the environment produced very numerous constraints on both governments and car manufacturers, also the cost of energy. It was found that the increase of valve lift is beneficial to performance (P , T , BMEP, BSFC and η_{vol}), but it is less effective at high valve lifts (over 10.5 mm), also IVO bTDC less than 25° is would reduce performance .

Keywords: variable valve timing, overlap angles, internal combustion engines, performance

Nomenclature

A	Coefficient in Wiebe equation, Annand open or closed cycle A coefficient	IVO	Inlet valve open, degree
$aBDC$	After Bottom Dead Center	k	Thermal conductivity of gas in the cylinder, W/m K
$BMEP$	Brake mean effective pressure, bar	M	Coefficient in Wiebe equation
$BSFC$	Brake specific fuel consumption, g/kWh	m_{frac}	Mole fraction
$bTDC$	Before Top Dead Center	NO_x	Nitrogen oxide
C	Carbon, Annand closed cycle coefficient	O_2	Oxygen
CO	Carbon monoxide	$Overlap$	Overlap, degree
CO_2	Carbon dioxide	P	Brake power, kW
c_p	Specific heat at constant pressure, kJ/kg K	Re	Reynolds number based upon mean piston speed and the engine bore
c_v	Specific heat at constant volume, kJ/kg K	T	Brake torque, N.m
D_{cyl}	Cylinder bore B, m	T_{gas}	Gas Temperature, Kelvin
dQ/A	Heat transfer per unit area, W/m ²	T_{wall}	wall Temperature, Kelvin
EVC	Exhaust valve close, degree	VVT	Variable valve timing
EVO	Exhaust valve open, degree	VL	Valve lift, mm
H	Hydrogen	η_{vol}	Volumetric Efficiency, %
h	Heat transfer coefficient, W/m ² K	Θ	actual burn angle, degree
IVC	Inlet valve close, degree	Θ_b	total burn angle (0-100%) burn duration),degree

Introduction

The control of green-house gas emissions has begun to add to the numerous constraints that vehicle manufacturers have to satisfy. The reduction of engine fuel consumption, gas motion within the cylinder is a major factor in the combustion process in SI engines , fuel-air mixing and heat transfer. [Haywood page 326]. As the valve is the minimum area of the flow , it has the highest velocity during the intake and the flow produce a shear layer. When dealing with engine topics exclusively, improving fuel economy to reduce CO₂ emissions means improving the engine thermal efficiency [1] .This target can be met following different routes, each of



them could be an effective way with different cost-to-benefit ratio. Often, it could be observed, it is helpful to adopt numerous solutions contemporaneously. As an example, fast combustion, lean burn, variable valve timing and actuation, gasoline direct injection and so long may be reminded. During most of its average life, a road engine is run under low load and low speed conditions. It is known that load reduction in spark-ignition engines is traditionally realized by introducing additional losses during the intake stroke by means of a throttle valve. In these operating points, the engine efficiency decreases from the peak values (already not very high) to values dramatically lower. The optimization of intake and exhaust valve timing can provide significant reductions in pumping losses at part load operation [2–4]. A number of papers have been sighted by [5]

Thermodynamic conditions during the closed cycle (compression, combustion and expansion) can be directly controlled by adjusting the intake valve opening IVO and closing angle (IVC), which defines the total intake mass flow rate and the effective compression ratio of the engine [6].

The objective of this paper is to contribute towards the development pursuing, among others on variable valve timing (VVT), for improving the engine performance. Furthermore, the investigation of the effect of valve lift at IVO, IVC and the Overlap angle between IVO and EVC on engine performance able to optimize engine torque and volumetric efficiency at the engine design speed. Power, BMEP and BSFC were calculated and presented to show the effect of varying valve lift timing on them for all the valve lift cases.

Theoretical analysis

For the purpose of analyzing the engine characteristics the dimensions were considered with a specially designed program used to predict the gas flows, combustion and overall performance of internal combustion engines. Engine speed was varied between 500 to 3500 rpm. Ignition was taken 10° bTDC.

Program Structure can be conceptualized as comprising three discrete modules.

The data entry and model generation are shown in Table (1).

Input data such as inlet pressure, temperature, equivalence ratio are also been introduced for all runs considered. Also the required exit data such as the back pressure are given.

The solution of the equations represents the physical processes to predict the flows between the elements of the model. It is designed to solve the energy, momentum and continuity equations as appropriate within each element to obtain the thermodynamic state variables and flow velocity at each crank angle throughout the engine cycle. The solution procedure is 'time marching' and a number of engine cycles are simulated in order to obtain a converged (cyclically repeatable) solution.

To simulate the engine the processes are broken down in such a way that a number of discrete sub-models such as the thermodynamic properties where the program tracks the flow of gas, as a mixture. For combustion the type of the fuel was as specified in Table (1). The effect of gas temperature on gas properties such as c_p , c_v and viscosity are calculated for the individual gas species and then 'averaged' using the Gibbs-Dalton relationships. Thus gas properties change appropriately with both gas composition and temperature.

Modeling the intake and exhaust ports of engines merely contains data relating to the valve flow coefficient at various valve lifts. The inlet throat gas velocity is calculated using the continuity equation. This considers the expanding volume of the cylinder as the piston moves down and calculates the corresponding velocity of the gas through the throat, assuming that the gas is an incompressible fluid.

When gas flows through a valve the development of separation and recirculation regions gives rise to a vena-contracta where the actual cross-sectional area of the gas stream (effective area) is less than the geometric area of the orifice. This phenomenon cannot be simulated directly using a one-dimensional model and has to be characterized using empirical data. Data giving measured effective valve areas, or flow coefficients (C_d). The effective area of a valve is a hypothetical concept which enables the mass flow through the valve to be evaluated for a given pressure difference across it. A mathematical model of the flow through the valve is developed, from which the 'effective' area of the valve throat can be derived from the measured values of pressure across the valve and the mass flow rates. The value of effective area obtained is dependent on the particular mathematical model (Woods and Khan [7]) and therefore if the data is to be supplied to a wave-action simulation program it is imperative that the model used to analyze the steady-flow data matches that employed in the boundary model of the computer program. In this way the use of effective flow area measured using a steady-flow rig enables the mass flow rate obtained in the experiments, for a particular valve lift and pressure difference across it.

Port flow database in which it was found that the inlet port flow coefficients at each valve lift / throat diameter ratio (L/D) are a function of the valve throat to bore area ratio.

The combustion process employed a single zone combustion model. The combustion rate defined via a one part *Wiebe* function. Dissociation effects (CO generation) were modeled through curve fits to the *Eltinge*



diagram, which relates combustion products of CO and O_2 to user specified parameters of air-fuel ratio and mal-distribution.

The *Wiebe* function define the mass fraction burned as

$$m_{\text{frac}} = 1.0 - \exp \left[-A \left(\frac{\theta}{\theta_b} \right)^{M+1} \right]$$

- A = coefficient in *Wiebe* equation = 10 for gasoline
 M = coefficient in *Wiebe* equation = 2.0 for gasoline
 θ = actual burn angle (after start of combustion) calculated by the program
 θ_b = total burn angle (0-100% burn duration)

Heat transfer was modeled in all elements. Within cylinders the empirically derived heat transfer correlation proposed by *Annand* was employed. It was chosen to be used in this analysis, the constant for such a case are available.

The connective heat transfer model proposed by *Annand* is defined as;

$$\frac{hD_{\text{cyl}}}{k} = A \text{Re}^B$$

Where

- h = heat transfer coefficient [$\text{W}/\text{m}^2 \text{K}$]
 A = *Annand* open or closed cycle A coefficient = 0.2
 B = *Annand* open or closed cycle B coefficient = 0.8
 k = thermal conductivity of gas in the cylinder [$\text{W}/\text{m K}$]
 D_{cyl} = cylinder bore $B=9.5$ [mm]
 Re = Reynolds number based upon mean piston speed and the engine bore. The density that calculated for the cylinder contents at each crank angle.

Thus the heat transfer per unit area of cylinder wall is defined as;

$$\frac{dQ}{A} = h(T_{\text{gas}} - T_{\text{wall}}) + C(T_{\text{gas}}^4 - T_{\text{wall}}^4)$$

Where:

- dQ/A = heat transfer per unit area [W/m^2]
 C = *Annand* closed cycle coefficient = 0 for the case considered.

The first part of the heat transfer equation is the connective heat transfer and the second part is the radiative heat transfer.

The outputs of the analysis and of the calculated results were given in an output file. Details of the element conditions and flows at each crank angle are stored for subsequent post processing. These results include in-cylinder pressures, temperatures, volumes and fuel mass fractions burned as well as all the input data of the test.

The IVO angle was varied while all other parameters were kept constant at different engine speeds collecting the results for further processing. Also the IVC angles were varied while other parameters were kept constant and it was also the case for overlap angle variation.

The exhaust gas emission produced due to engine run, at the design speed of 2500 rpm, was investigated using the engine data and fuel utilized. The combustion pressures attained and the fuel air ratio used was fed to the Engineering Equation Solver software EES and the values of mole fraction of NO , CO , CO_2 , H_2O , O_2 and N_2 were recorded and later plotted for all cases considered.

Results

Effect of valve lift on IVO angle

Inlet valve opening angle (IVO) effect



For the engine geometry and running conditions shown above, all parameters were kept constant except the IVO angle and the valve lift value. The IVO was varied from the original value 54° IVO angle bTDC opening down to 0° at TDC in steps for three valve lift values. As shown in Figure (1) the brake power is drawn versus the IVO angle opening bTDC for different valve lifts from (8.5, 9, 9.5, 10 and 10.5 mm) at the engine design speed ($N_d = 2500$ rpm). It showed an increase in power with the IVO angle reduction but this increase in power was small for values of IVO angle bTDC less than 25° for all engine running speeds considered. The increase in power may be due to the reduction of residual gases and backflow of exhaust into the inlet manifold. The reduction of valve lift show a considerable reduction in power may be due to the restriction on charge gas inflow to the cylinder, may be due to the viscous effect of the attached jet formed by the low lift valve which is Reynolds number dependent [9], while the increase of valve lift shows an increase in power over the original 9.5 mm lift as they produce a larger effective area [8].

Figure (2) shows the variation of torque versus IVO angle bTDC at different valve lifts. The late opening of inlet valve showed an increase in brake torque especially at higher valve lifts. A less effect on torque at IVO angles less than 20°. It shows a similar behavior of the considerable decrease in torque due to the decrease in valve lift and the slight increase due to increase in valve lift.

Figure (3) shows the variation of BMEP versus IVO angle bTDC which behave similar to the Torque behavior it showed an increase in BMEP with less IVO angle bTDC than the original one also an increase with increasing valve lift. This was also noticed by [1] as the BMEP increase by decreasing the IVO angle bTDC.

Figure (4) shows the variation of BSFC versus IVO angle bTDC; this showed that BSFC is hardly affected by IVO angle bTDC higher than 20° for different valve lifts. But it shows an increase in BSFC for all valve lifts at IVO angles less than 20°.

Figure (5) showed the effect of IVO angle bTDC on volumetric efficiency η_{vol} . This show a noticeable increase in volumetric efficiency η_{vol} with reducing IVO angle bTDC for all valve lifts considered where it showed a slight decrease at IVO angle bTDC less than 20°. Early IVO angle bTDC cause the high pressure exhaust gas reducing the amount of inlet mixture incoming through the inlet manifold this is quite noticed at high valve lifts on early IVO opening where a large effective flow area is present [8].

Inlet valve closing angle (IVC) effect

For the engine geometry and running conditions shown above, all parameters were kept constant except the IVC angle and the valve lift. It was varied from the original value 22° IVC angle aBDC opening down to 0° at BDC in steps for different valve lifts values. Figure (6) show the brake power drawn versus the IVC angle closing aBDC for valve lifts (8.5, 9, 9.5, 10 and 10.5 mm) at the engine design speed ($N_d = 2500$ rpm). It showed a decrease in power with the IVC angle reduction for all valve lifts considered. But it is less sever at higher valve lifts. That was noticed by [4], he shows that, a late IVC reduce the volumetric efficiency. In contrast early IVC leads to greater reduction in volumetric efficiency, and this limits the output power. Also [10] noted that the late closing of the intake valve, long after the BDC, leads to a higher cylinder charge.

Figure (7) shows the variation of torque versus IVC angle aBDC at different valve lifts. The late closing of the inlet valve close aBDC showed an increase in brake torque for all valve lifts and of nearly similar trends but with a less effect at high lifts.

Figure (8) shows the variation of BMEP versus IVC angle aBDC, this showed that BMEP decreases with reducing IVC angle aBDC values for valve lifts and they nearly have a similar trend also.

Figure (9) shows the variation of BSFC versus IVC angle aBDC; this showed that BSFC is slightly affected by IVC angle aBDC, as it is increased slightly by reducing IVC angle aBDC.

Figure (10) showed the effect of IVC angle aBDC on volumetric efficiency η_{vol} . This shows a noticeable decrease in volumetric efficiency η_{vol} with reducing IVC angle aBDC, especially at lower valve lifts This was also noticed by [8], which will lead to limit the maximum power output.

Overlap angle (IVO – EVC) effect

For the engine geometry and running conditions shown above, all parameters were kept constant except the overlap angle between IVO and EVC at TDC and valve lifts. The former was varied from the original value 108° overlap angle at TDC down to 0° at TDC in steps while for the later three values were considered (8.5, 9, 9.5, 10 and 10.5 mm). Figure (11) shows the brake power drawn versus the overlap angle at TDC. For all valve lifts the power showed an increase with reducing overlap angle till about 60° angle then it starts a considerable decrease to lower values at 0° overlap. It has a larger reduction for less valve lifts considered



Figure (12) shows the variation of torque versus overlap angle at TDC. The decrease in overlap angle between IVO and EVC showed an increase in torque to reach a maximum value then a decrease at overlap angle 0° , both at high overlap angles and high valve lifts. But at lower valve lifts has a more sever effect.

Figure (13) shows the variation of BMEP versus overlap angle at TDC, this showed that BMEP have a similar trend as the torque with overlap angle at TDC values for all valve lifts and they nearly have a similar trend also. But the effect at high overlap angles and at high valve lifts is less sever and low valve lift has a more sever effect.

Figure (14) shows the variation of BSFC versus overlap angle at TDC, this showed that BSFC decreases to a minimum at lower overlap angles at TDC then an increase toward the 0° overlap angle. This is quite noticeable at low valve lifts while it approaches a minimum at around overlap angle around 60° .

Figure (15) shows the effect of overlap angle at TDC on volumetric efficiency η_{vol} . This shows a noticeable increase in volumetric efficiency η_{vol} with reducing overlap angle at TDC,. The maximum was at higher overlap angles at high valve lifts than at lower ones. This is due to the eliminating of the left residuals in the cylinder from the previous cycle; also this was noticed by [9], where the valve overlap permits exhaust action to assist the intake and improve the volumetric efficiency.

Engine emission

Figure (16) shows the effect of IVO angle bTDC on NO emission at the design speed (2500 rpm) for different valve lifts only (8.5, 9.5 and 10.5 mm) were selected for the presentation. The reduction of IVO angle causes a further reduction of NO mole fraction down to angle 10° bTDC. The reduction in NO is quit noticeable with increasing the valve lift to 10.5 mm.

Figure (17) shows the effect of IVC angle bTDC on NO emission at the design speed (2500 rpm) for different valve lifts. An ever increase in NO with the reduction of IVC angle down to 0° .

Figure (18) shows the effect of overlap angle bTDC on NO emission at the design speed (2500 rpm) for different valve lifts. A reduction in NO could be recognized for all valve lifts down to 60° then a sharp increase in NO as the overlap angle is reduced.

Figure (19) shows the effect of IVO angle bTDC on CO emission at the design speed (2500 rpm) for different valve lifts. The reduction of IVO angle causes a further reduction of CO mole fraction down to angle 10° bTDC.

Figure (20) shows the effect of IVC angle bTDC on CO emission at the design speed (2500 rpm) for different valve lifts. An ever increase in CO with the reduction of IVC angle down to 0° similar to NO behavior.

Figure (21) shows the effect of overlap angle bTDC on CO emission at the design speed (2500 rpm) for different valve lifts. A reduction in CO could be recognized for all valve lifts down to 60° then a sharp increase in CO as the overlap angle is reduced.

Values of other parameters were hardly altered like CO_2 and H_2O .

Conclusions

1. Increasing the valve lift is beneficial to engine performance, its effect is more apparent at low IVO angles were a better performance is indicated.
2. Volumetric efficiency appeared to be hardly effected when valve lifts are high.
3. For all valve lifts the decrease in IVC angle would reduce engine performance.
4. A small effect of valve lift was noticed at high overlap angle case, but this effect is noticed when reducing this angle.
5. Engine emission (NO and CO) is reduced through the increase of the valve lift for all cases studied.

References

1. Fontana, G., Galloni, E. , "Variable valve timing for fuel economy improvement in a small spark-ignition engine"; Applied Energy 86 (2009) 96–105
2. Ahmad, T. and Thobald, MA., "A survey of variable valve actuation technology"; SAE, New York, SAE paper 89, 674, 1989.
3. Gray, C., "A review of variable engine valve timing"; SAE, New York, SAE paper, 880 386, 1988.



- Shiga, S., Yagi, S., Morita, M., Matsumoto, T., Karasawa, T., and Nakamura, T. "Effects on valve close timing for internal combustion engines"; Trans Jpn Soc Mech. Eng Ser B 1996;62(596):1659-65.
- Kosuke, N., Hiroyuki, K. and Kazuya, K.; " Valve timing and valve lift control mechanism for engines" ;Mechatronics 16 (2006) 121-129
- Benajes, J., Molina, S., Martin, J. and Novella, R. , "Effect of advancing the closing angle of the intake valves on diffusion-controlled combustion in a HD diesel engine"; Applied Thermal Engineering 29 (2009) 1947-1954
- Woods, W.A. and Khan, S.R. An experimental study of flow through poppet valves. Proc.I.Mech.E. Vol. 18 No.32, (1965-66).
- R. Stone, "Introduction to Internal Combustion Engines"; McMillan Press, 3rd edition, London, 1999.
- Baur, H., "Gasoline-engine Management - Basic components"; Bosch Company, 1st edition, Stuttgart, 2001.
- Ferguson, R. C. and Kirkpatrick, A. T.; "Internal combustion engines Applied thermodynamics", 2nd Edition, John Wiley and sons inc., New York, 2001.

Variable Geometry Different Throat Diameter RPM = 2500 IVO effect on valve lift

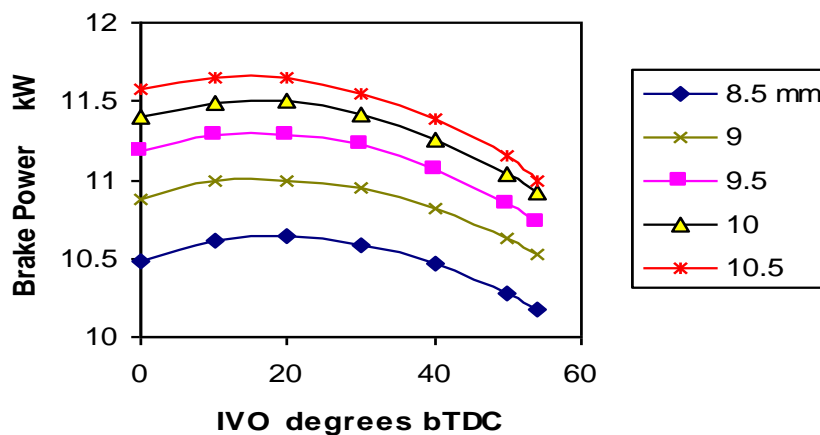


Figure (1) Power versus IVO angle at different valve lifts ($N_{\text{disg}}=2500$ rpm)

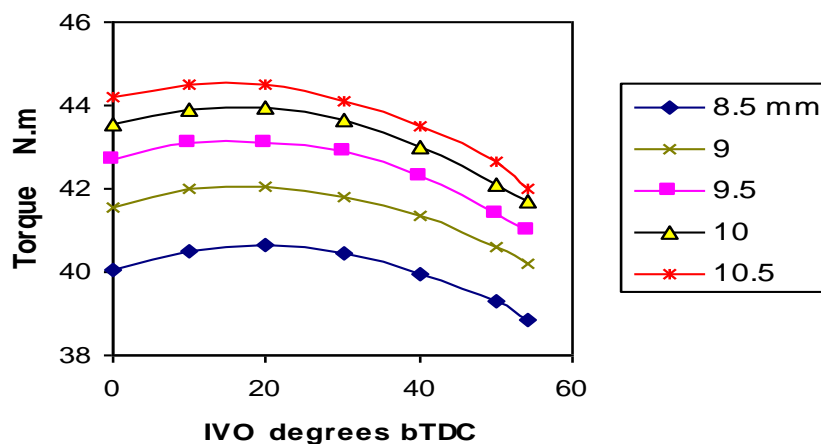


Figure (2) Torque versus IVO angle at different valve lifts ($N_{\text{disg}}=2500$ rpm)

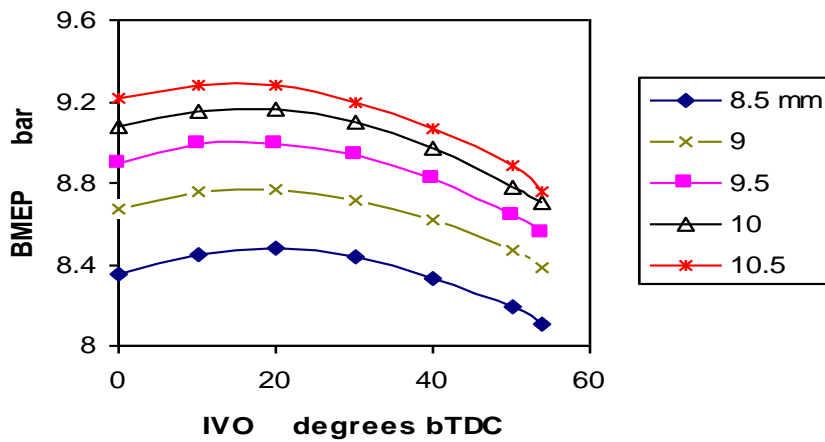


Figure (3) BMEP versus IVO angle at different valve lifts ($N_{disg} = 2500$ rpm)

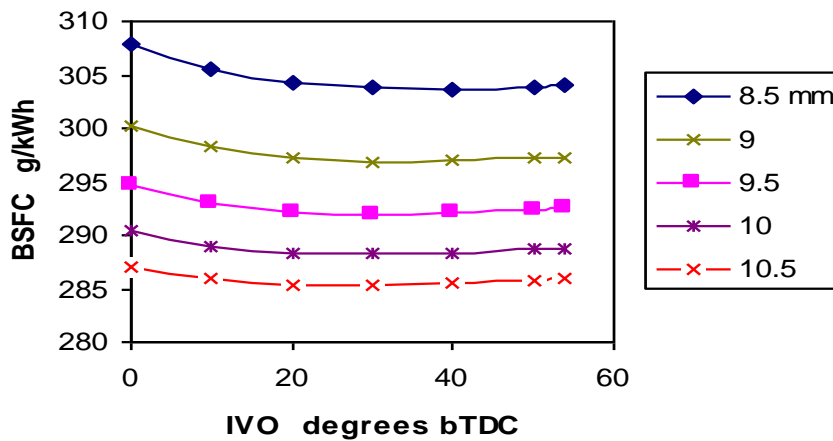


Figure (4) BSFC versus IVO angle at different valve lifts ($N_{disg} = 2500$ rpm)

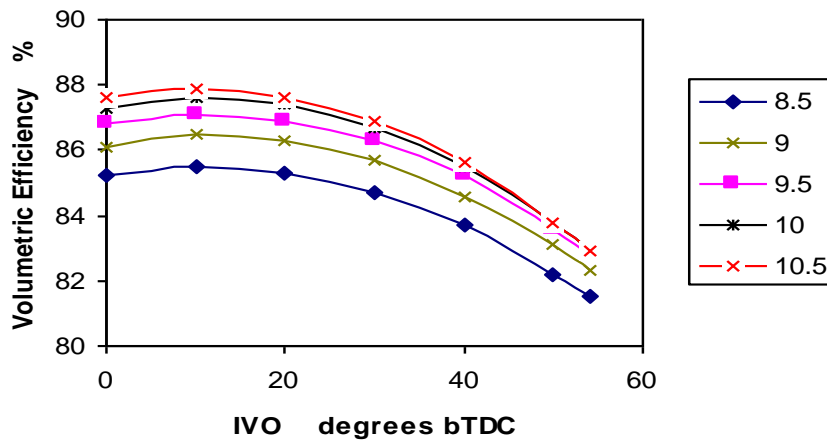


Figure (5) Volumetric efficiency versus IVO angle at different valve lifts



($N_{\text{disg}} = 2500 \text{ rpm}$)

IVC effect on valve lift

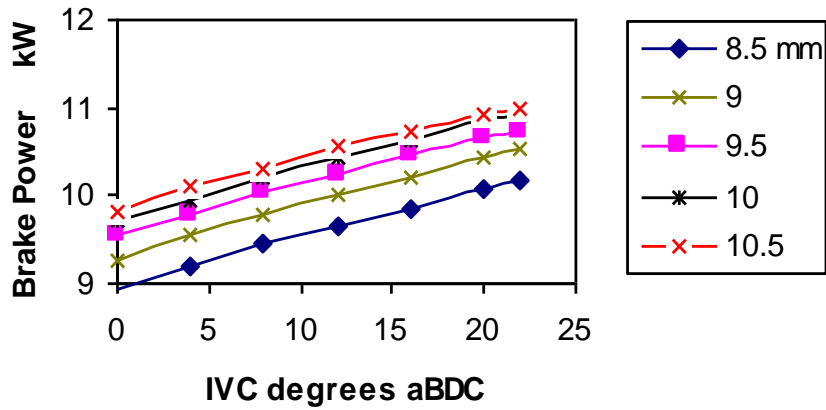


Figure (6) Power versus IVC angle at different valve lifts ($N_{\text{disg}} = 2500 \text{ rpm}$)

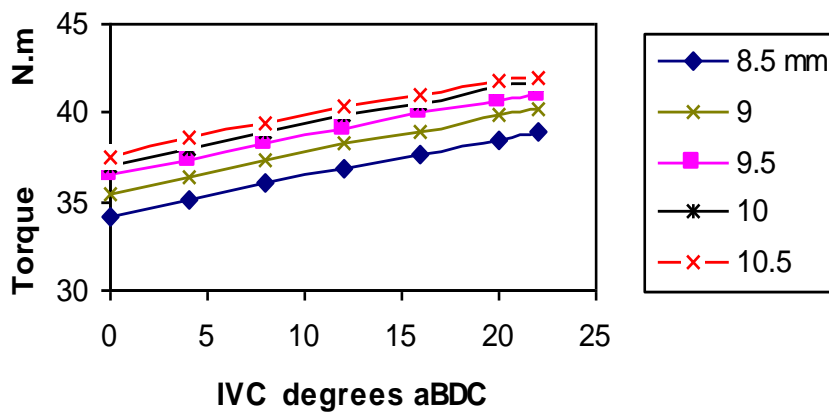


Figure (7) Torque versus IVC angle at different valve lifts ($N_{\text{disg}} = 2500 \text{ rpm}$)

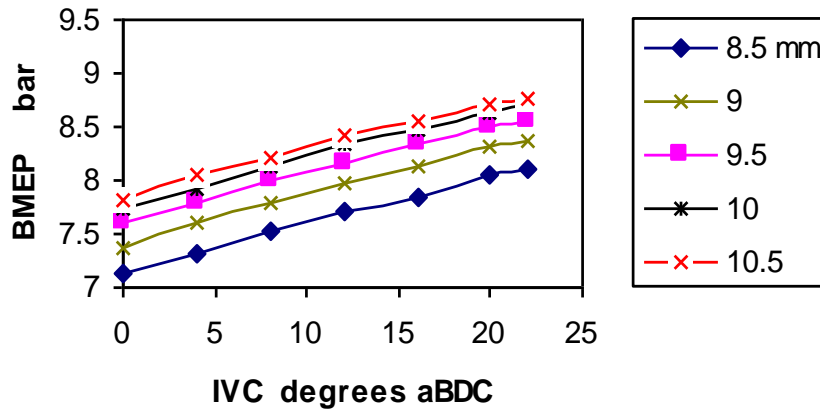


Figure (8) BMEP versus IVC angle at different valve lifts ($N_{disg} = 2500$ rpm)

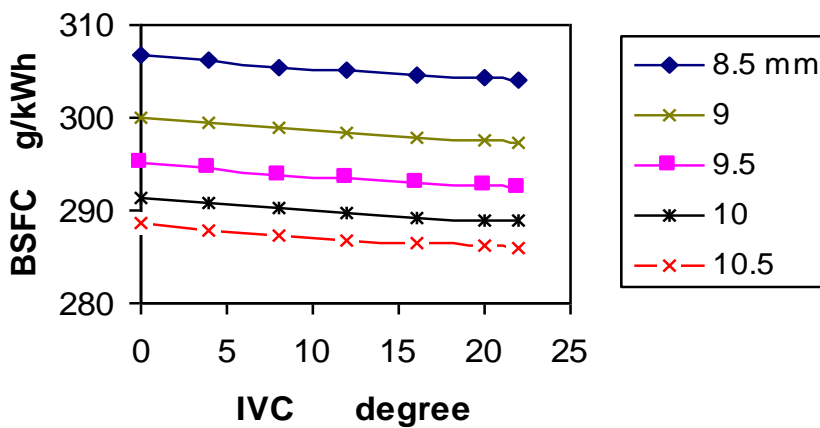


Figure (9) BSFC versus IVC angle at different valve lifts ($N_{disg} = 2500$ rpm)

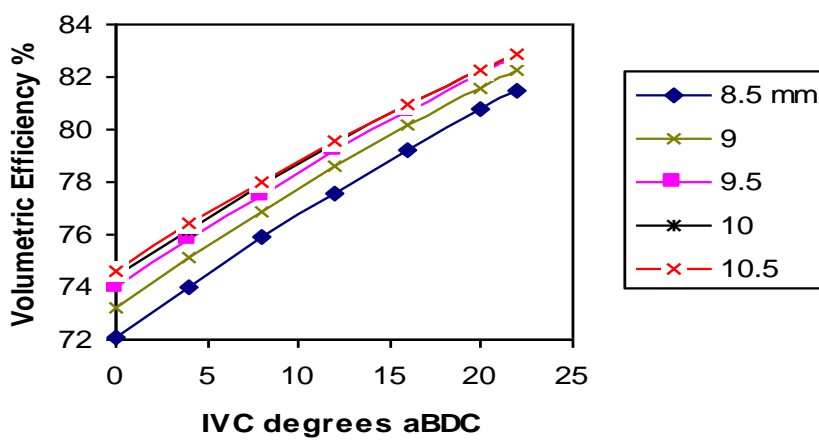


Figure (10) Volumetric efficiency versus IVC angle at different valve lifts
($N_{disg} = 2500$ rpm)



Overlap effect on valve lift

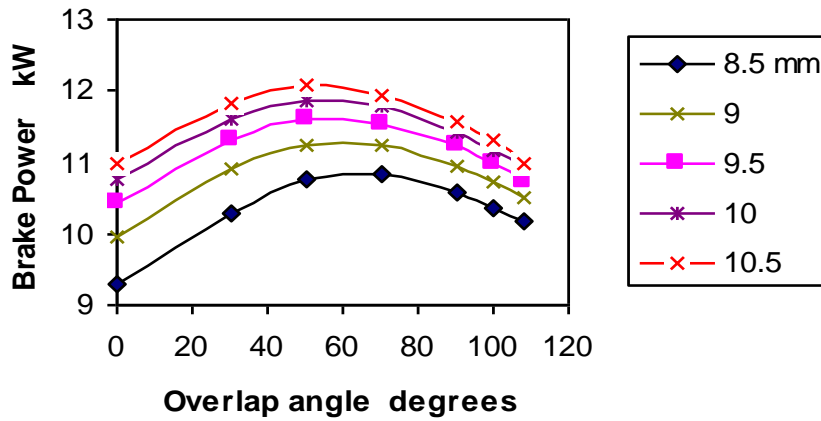


Figure (11) Power versus overlap angle at different valve lifts ($N_{\text{disg}} = 2500$ rpm)

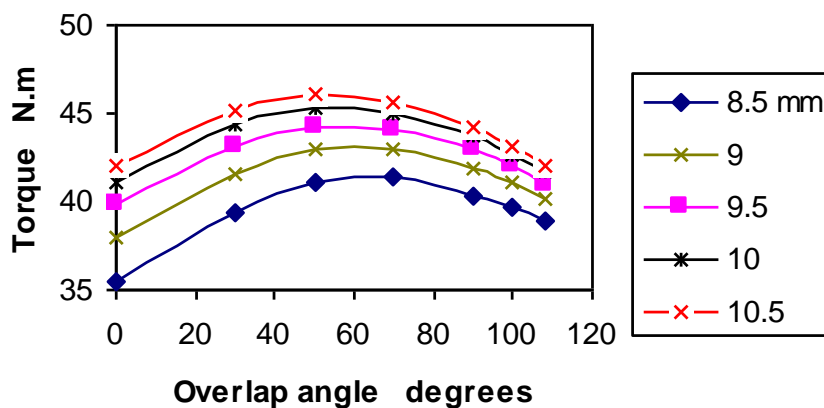


Figure (12) Torque versus overlap angle at different valve lifts ($N_{\text{disg}} = 2500$ rpm)

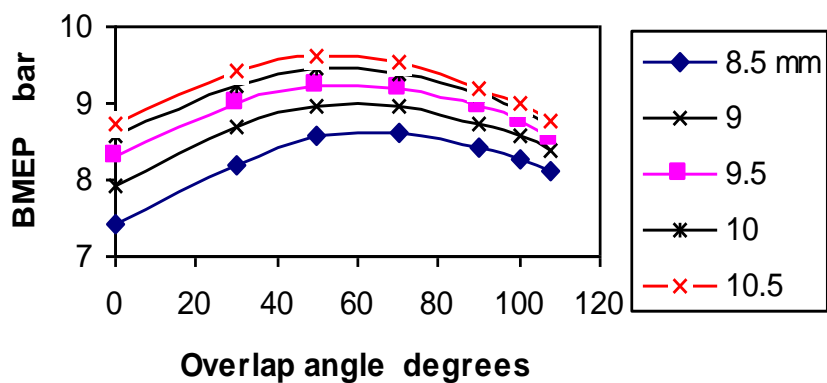


Figure (13) BMEP versus overlap angle at different valve lifts ($N_{\text{disg}} = 2500$ rpm)

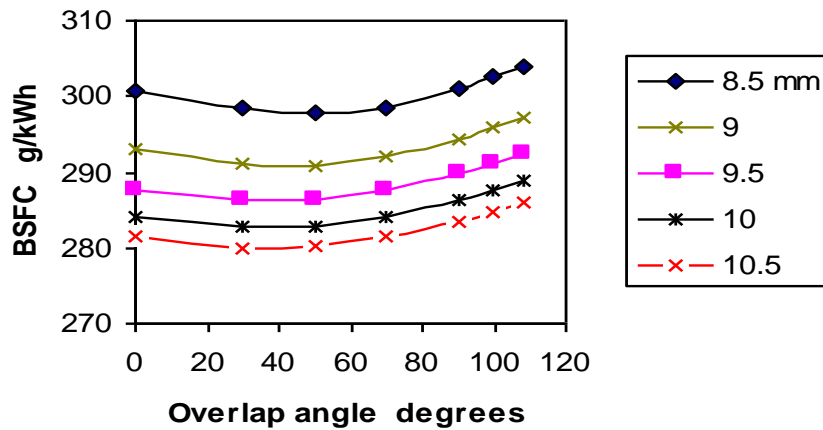


Figure (14) BSFC versus overlap angle at different valve lifts ($N_{disg}=2500$ rpm)

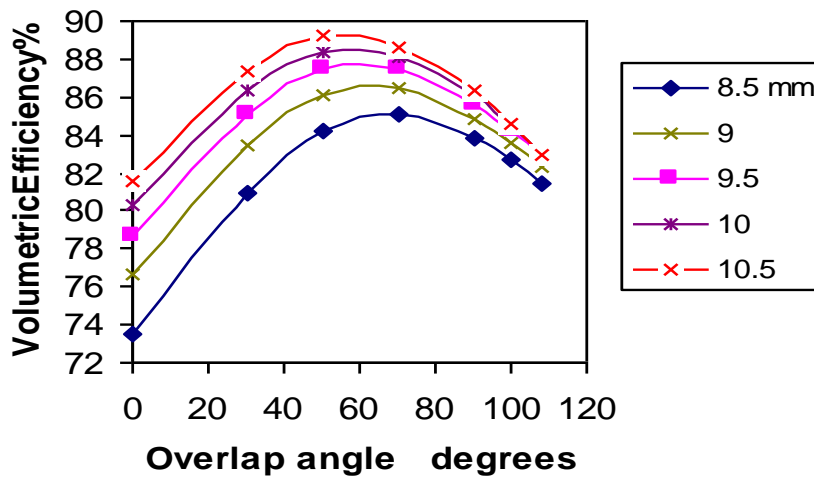


Figure (15) Volumetric efficiency versus overlap angle at different valve lifts ($N_{disg}=2500$ rpm)

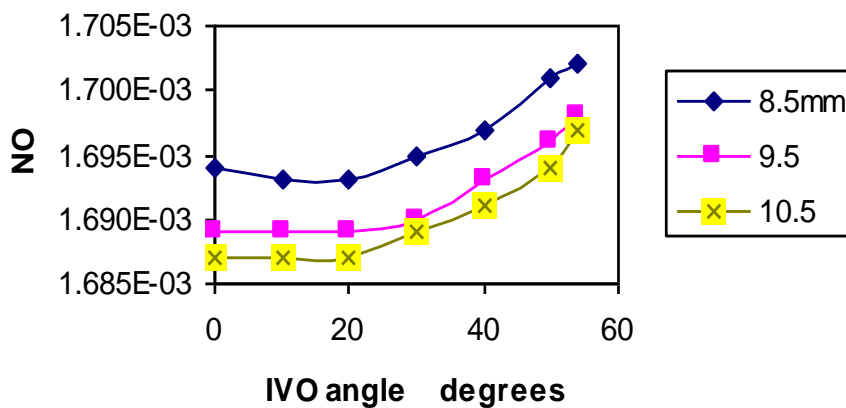


Figure (16) NO versus IVO angle at different valve lifts ($N_{disg}=2500$ rpm)

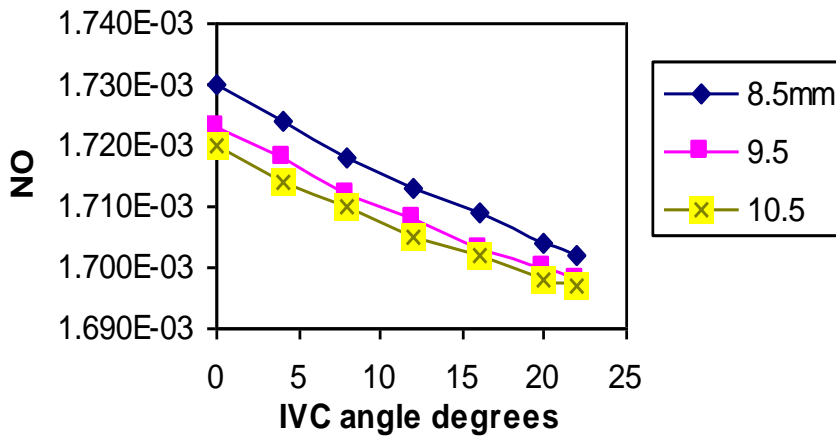


Figure (17) NO versus IVC angle at different valve lifts ($N_{disg} = 2500$ rpm)

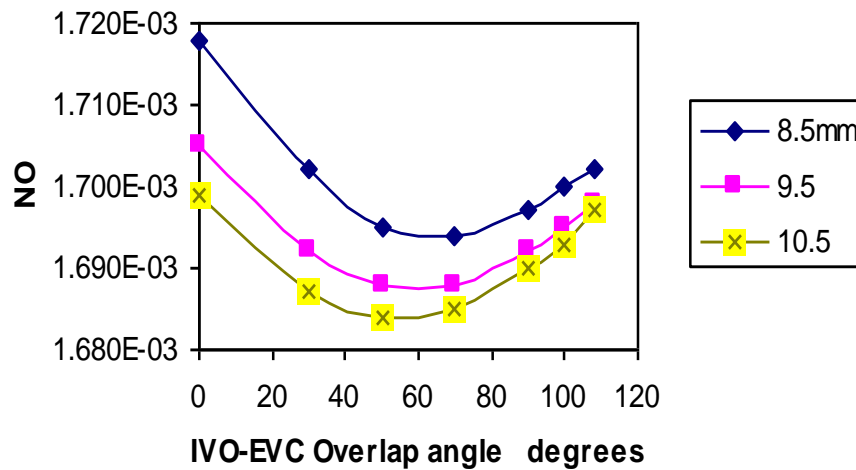


Figure (18) NO versus Overlap angle at different valve lifts ($N_{disg} = 2500$ rpm)

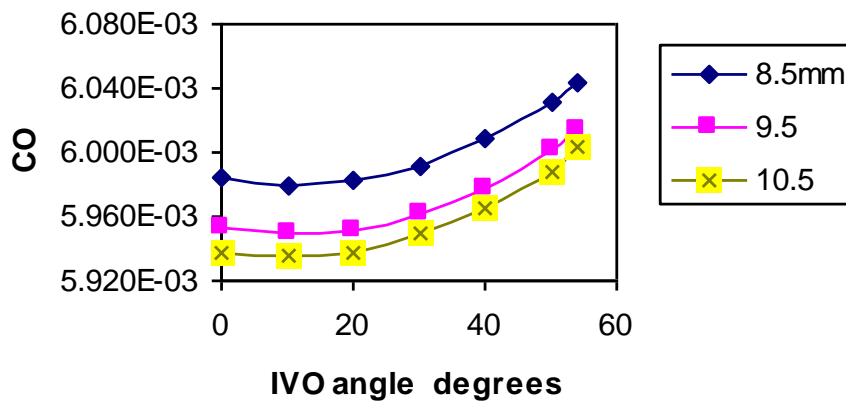


Figure (19) CO versus IVO angle at different valve lifts ($N_{disg} = 2500$ rpm)

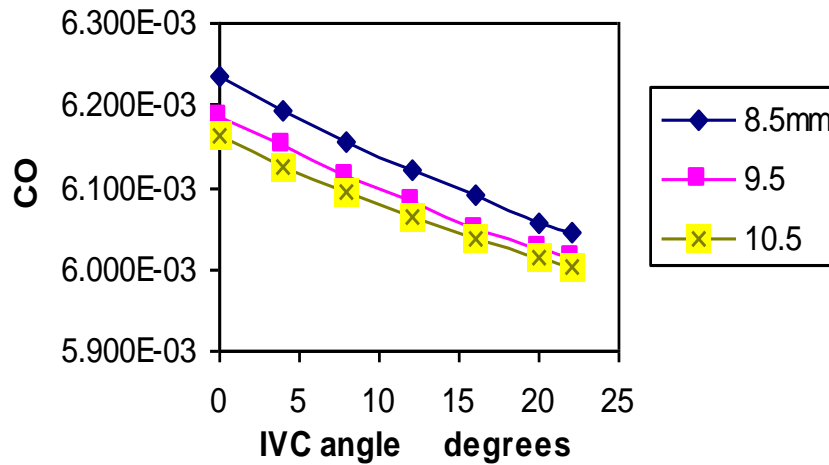


Figure (20) CO versus IVC angle at different valve lifts ($N_{disg} = 2500$ rpm)

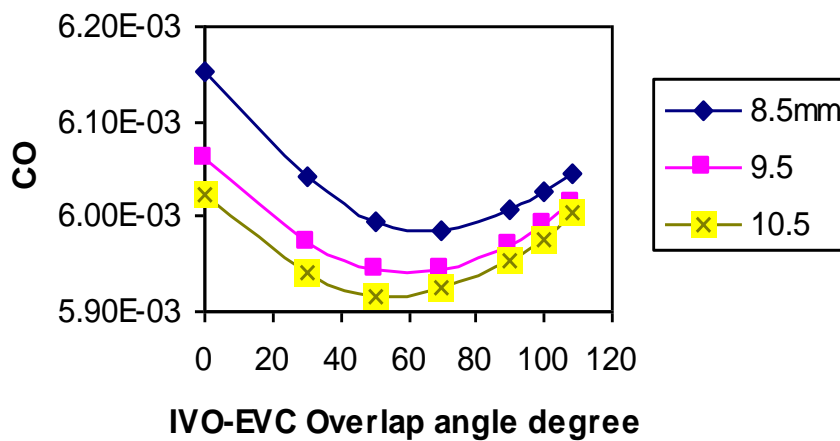


Figure (21) CO versus Overlap angle at different valve lifts ($N_{disg} = 2500$ rpm)

Table (1) Base Engine Data

No. of cylinders	Bore	Stroke	Connecting rod length	compression ratio
1	95 mm	85 mm	129.8 mm	8

Fuel type is Iso-Octane (C₈H₁₈) of the following properties:

Heating value	Density	H/C molar	molecular mass
43000 kJ/kg	0.75 kg/liter	1.8	114.23kg/k.mol

Valves data are as follows considering single valve for inlet and exhaust valves. The original valve timing, inlet throat diameter and valves lift are:

IVO angle	IVC	EVO	EVC	inlet throat dia.	exhaust throat dia.	valves lift
54° bTDC	22° aBDC	22 bBDC,	54 aTDC	31 mm	26 mm	9.5 mm



The 7th Jordanian International Mechanical Engineering Conference (JIMEC'7)
27 - 29 September 2010, Amman – Jordan
